

# TRACE ELEMENT AND Pb ISOTOPE GEOCHEMISTRY OF TISSINT IMPACT MELT GLASS AND SULFIDE

## REVEAL NO CONTAMINATION BY MARTIAN SOIL



T. J. Lapen<sup>1</sup>, S. E. Suarez<sup>1</sup>, M. Richter<sup>1</sup>, A. J. Irving<sup>2</sup>, K. Richter<sup>3</sup>,  
<sup>1</sup>Dept. Earth and Atm. Sci., University of Houston, Houston, TX (tjlapen@uh.edu)  
<sup>2</sup>Department of Earth and Space Sciences, University of Washington, Seattle WA  
<sup>3</sup>NASA Johnson Space Center, Houston, TX



### Tissint impact melt includes soil?

- The impact glass within shergottites EETA 79001 and Tissint have been hypothesized to contain martian soil components incorporated during the shock ejection event [1,2], but this hypothesis has been debated [3].
- Predicted signatures of a soil component include enrichment in S [1] and trace elements, such as light rare earth elements (LREE), Ba, Th [1,2]. Soil will have more radiogenic Sr, Pb, and Os, and less radiogenic Nd and Hf isotopic compositions than sources of depleted shergottites.
- Despite the clear evidence for Mars atmospheric components in impact glass, incorporation of a crustal component has been difficult to definitively test.

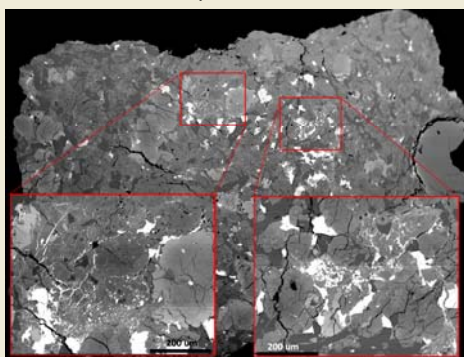


**Figure 1.** SEM-BSE images of the analyzed fragment. The bright phases are pyrrhotite (as intact grains and as veins and droplets), large phenocrysts are olivine, light grey areas associated with sulfide veins and areas without distinct igneous textures are impact glass, light and dark gray grains in the groundmass are pyroxene and maskelynite, respectively.

### In this study:

- A polished 1.5 x 2.0 mm impact glass and sulfide-rich fragment of Tissint (Fig. 1; Sample TS2 [5]) was analyzed *in situ* for REE and highly siderophile element (HSE) concentrations and Pb isotopic compositions.
- The data are used to assess whether the sulfide-rich impact melt glass in Tissint contains any detectable exogenous components.

### Analytical Methods

- SEM BSE images were acquired at UH-TcSUH.
- Laser ablation analysis utilized a **Teledyne-Cetac Analyte Excite** coupled to a **Varian 810** quadrupole ICPMS at UH.
- Each 65-85µm spot analysis was conducted at 10-25 Hz repetition rates, a fluence of 4 J/cm<sup>2</sup>, 30s on-peak blank, 30s ablation time. **Operating conditions of the samples were exactly matched to the standards for each analysis.**
- Calibration standards include **NIST 612 glass** (Pb isotopes), **BHVO-2G** (REE concentrations), and the **HOBA** meteorite (HSE concentrations). External standards were **BHVO-2G** (Pb), **BIR-1G** (REE), and **Filomena** (HSE).

- Pb data were corrected for the <sup>204</sup>Hg isobar in the instrument blank and Hg in the standards by monitoring <sup>201</sup>Hg and <sup>202</sup>Hg; other Pb isotope data reduction methods follow [6]. Trace element concentrations were processed using the *Glitter* program.

### Results

- The REE concentrations of Tissint glass, sulfide, and mixtures are summarized in Fig. 2.

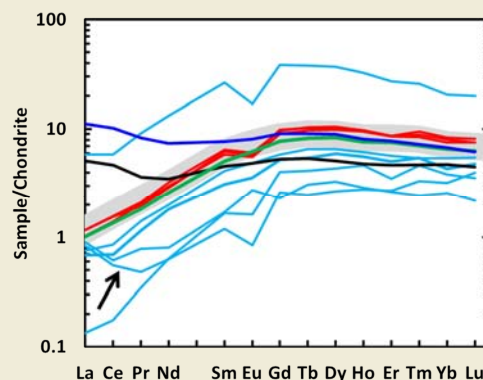


**Figure 2.** Chondrite-normalized REE for Tissint whole rock (light grey) [3,8], impact glass (green [3]; black [2]; red, this study), 'groundmass' (dark blue) [2], sulfide and sulfide + glass (light blue, this study). Arrow points to LREE enrichment for some analyses.

- Pb isotopic compositions of BHVO-2G, which had similar concentrations of Pb (1.7 ppm) as the sulfide and impact glass, yielded <sup>206</sup>Pb/<sup>204</sup>Pb = 18.92 ± 0.47, <sup>207</sup>Pb/<sup>204</sup>Pb = 15.77 ± 0.48, <sup>208</sup>Pb/<sup>204</sup>Pb = 38.87 ± 1.10, and <sup>207</sup>Pb/<sup>206</sup>Pb = 0.8335 ± 0.0092, which are identical to the accepted GeoReM values within uncertainty. (n=10; 2SD).
- Pb isotopic compositions of Tissint samples are summarized in Fig. 3; all data yielded the following weighted averages (n=11; 2SD):

$$\begin{aligned}^{206}\text{Pb}/^{204}\text{Pb} &= 10.42 \pm 0.30 \\ ^{207}\text{Pb}/^{204}\text{Pb} &= 10.88 \pm 0.30 \\ ^{208}\text{Pb}/^{204}\text{Pb} &= 29.46 \pm 0.93 \\ ^{207}\text{Pb}/^{206}\text{Pb} &= 1.043 \pm 0.018\end{aligned}$$

- The <sup>238</sup>U/<sup>204</sup>Pb ratio for the glass and sulfide average 0.1 ± 0.1 (1SD), so no age correction is necessary.

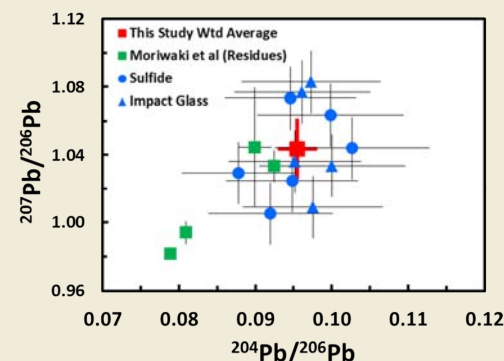


**Figure 3.** Measured Pb isotopic compositions of sulfide and impact glass. Weighted average based on the 11 blue data points. All errors are 2SD. Green data from [7].

- The HSE data and concentration patterns (Fig. 4) are compared to Tissint whole rock and HSE concentrations of 'intermediate MgO' shergottite whole rocks [8].

### Results continued

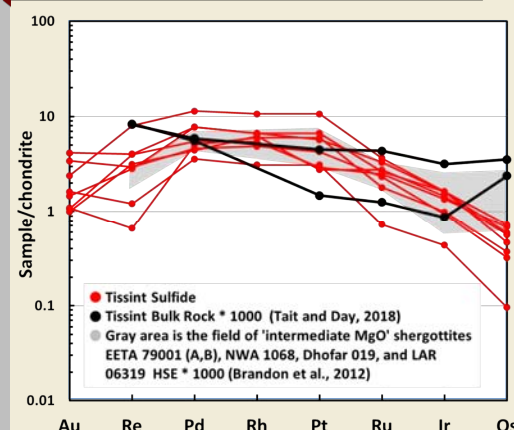


**Figure 4.** HSE data of Tissint sulfides (Red) compared to 1000 times the concentrations of Tissint bulk rock (black) [9] and the field of 'intermediate MgO' shergottites [8].

### Discussion and Conclusions

- REE data of impact melt glass (red, Fig. 2) are identical to the bulk rock and impact glass of [3] except that our sample contains a negative Eu anomaly. Some of the sulfide rich material shows an enrichment in LREE, similar but less in magnitude to that observed by [2].
- The Pb isotopes are nearly identical to the least radiogenic values measured by [5], which reflect the mantle source compositions. These values represent some of the least radiogenic Pb for any shergottite with the exception of NWA 7635 [10], and are inconsistent with ancient evolved crust.
- The HSE data of the sulfides show a pattern consistent with HSE fractionation during igneous petrogenesis [9-11]. The patterns and HSE ratios are consistent with patterns of 'intermediate MgO' shergottites [10].
- In summary, **in situ analyses of Tissint impact glass and associated sulfide provide no evidence for exogenous materials. The host of labile radiogenic Pb and Sr [e.g., 5,7] is unrelated to the impact melt glasses and instead are likely related to mineral film coatings, and at least for labile Sr, is likely related to nearby depleted shergottite rock units on Mars [5].**

**References:** [1] Rao et al. (2018) *MAPS*, 53, 2558-2582. [2] Chennaoui Aoudjehane H. et al. (2012) *Science*, 338, 785-788. [3] Barrat et al. (2014) *GCA*, 125, 23-33. [5] Suarez et al. (This Meeting). [6] Shaull et al. (2010) *G-cubed*, 11. [7] Moriwaki et al. (2018) *EPSL*, 474, 180-189. [8] Brandon et al. (2012) *GCA* 76, 206-235. [9] Tait and Day (2018) *EPSL*, 494, 99-108. [10] Andreasen et al. (2014) *LPS*, 45, abstract #2365 [11] Baumgartner et al. (2017) *GCA*, 210, 1-24.

**Acknowledgements:** We thank the NASA Solar Systems Workings Program award 80NSSC18K0333 for project funding.